

Article

A New Intelligent Dynamic Control Method for a Class of Stochastic Nonlinear Systems

Haifeng Huang ^{1,*}, Mohammadamin Shirkhani ^{2,*} , Jafar Tavoosi ²  and Omar Mahmoud ³¹ School of Electrical and Information Technology, Zhenjiang College, Zhenjiang 212028, China² Department of Electrical Engineering, Ilam University, Ilam 69315-516, Iran; j.tavoosi@ilam.ac.ir³ Faculty of Engineering and Technology, Future University in Egypt, New Cairo 11835, Egypt; omar.saad@fue.edu.eg

* Correspondence: beiquexin@163.com (H.H.); mohammadaminshirkhani77@gmail.com (M.S.)

Abstract: This paper presents a new method for a comprehensive stabilization and backstepping control system design for a class of stochastic nonlinear systems. These types of systems are so abundant in practice that the control system designer must assume that random noise with a definite probability distribution affects the dynamics and observations of state variables. Stochastic control is intended to determine the time course of control variables so that the control target is achievable even with minimal cost. Since the mathematical equations of stochastic nonlinear systems are not always constant, not every model-based controller can be accurate. Therefore, in this paper, a type-3 fuzzy neural network is used to estimate the parameters of the backstepping control method. In the simulation, the proposed method is compared with the Type-1 fuzzy and RBFN methods. Results clearly show that the proposed method has a very good performance and can be used for any system in this class.



Citation: Huang, H.; Shirkhani, M.; Tavoosi, J.; Mahmoud, O. A New Intelligent Dynamic Control Method for a Class of Stochastic Nonlinear Systems. *Mathematics* **2022**, *10*, 1406. <https://doi.org/10.3390/math10091406>

Academic Editor: Georgios Tsekouras

Received: 15 March 2022

Accepted: 12 April 2022

Published: 22 April 2022

Publisher's Note: MDPI stays neutral with regard to jurisdictional claims in published maps and institutional affiliations.



Copyright: © 2022 by the authors. Licensee MDPI, Basel, Switzerland. This article is an open access article distributed under the terms and conditions of the Creative Commons Attribution (CC BY) license (<https://creativecommons.org/licenses/by/4.0/>).

Keywords: parameter estimation; stochastic systems; type-3 fuzzy neural network; backstepping control method

MSC: 13P25

1. Introduction

The essence of most real and physical systems is nonlinear. This nonlinear dynamic behaviour complicates control systems, especially when hysteresis phenomena are taken into account [1–3]. In recent years, nonlinear systems have received a lot of attention and many efforts have been made to stabilize them. One of the root causes of instability in systems is related to their nonlinear nature (dynamics), to which the designer of the control system must pay special attention [4–8]. Hence, innovative techniques in [9] are proposed to achieve a systematic design procedure for these highly nonlinear systems, including the backstepping design method. Due to the increasing complexity of the problem, these systems are classified into the following three classes of systems: strict feedback systems, pure feedback systems, and block strict feedback systems. In [10], using the backstepping method, and in combination with the radial basis function neural network (RBFN), a creative controller was designed for strict feedback nonlinear stochastic systems with unknown dynamics. There is a so-called “explosion of complexity”, which complicates the design and simulation by increasing the system rank. A very creative technique called dynamic surface control (DSC) is suggested in [11], which can prevent disturbing phenomena. Numerous studies [7–11] use this technique instead of using the backstepping design method, in order to prevent the occurrence of the phenomenon of an “explosion of complexity”, and they have proposed some methods to stabilize different forms of nonlinear systems. Some of these studies will be reviewed in the following. In [12], with the development of a dynamic level control method using Gaussian networks, a controller

for non-linear toxins in the form of strict feedback with desired indeterminacy is presented. In [13], the problem of adaptive tracking control for a class of indeterminate strict single input–single output with unknown path and control perturbations is investigated, and the DSC design method is used to solve the “explosion of complexity” problem. In [14], a creative controller is presented based on a combination of the dynamic surface control and adaptive fuzzy sliding mode control method for a MEMS gyroscope. In [15], the dynamic surface control, considering the saturation, is presented for the problem of safe entry into the spacecraft terminal based on the spacecraft’s relative motion model and the potential to prevent the collision of the sphere. Occurrence of failure in control systems can lead to catastrophic accidents. Therefore, many efforts have been made to prevent the occurrence of such accidents, and to deal with adverse effects on control systems. Malfunctions may occur in various parts of a control system, from the attack of sensors, actuators, controllers, communication lines, and so on. Among the topics of interest to researchers in recent years is the occurrence of malfunctions in control system cells. Actuator failure means changing the characteristic of the actuator from a linear state to a variety of nonlinear states, including the actuator’s physical performance, its jamming, the dead-zone phenomenon, the residual phenomenon in the actuator, and so on. In the following, studies will be reviewed that have examined the occurrence of each of these types of defects in the actuators. In [16], DSC has been used to avoid the “explosion of complexity” phenomenon in a conventional backstepping method, and then, by introducing the Lyapunov integral function, they provide a controller for pure feedback nonlinear systems with a dead-zone area. In [17], the occurrence of variable failures in nonlinear systems has been investigated. They proposed an adaptive synchronization sliding mode technique to solve the problems caused by uncertain system parameters, actuator failure, and perturbations. In [18], the problem of adaptive control for stochastic nonlinear systems with time delay and a dead-zone is investigated. In the aforementioned paper, they used an adaptive control scheme based on neural networks, DSC, and a minimum learning parameters algorithm. In order to reduce the complexity of the calculations, a creative controller has also been proposed to eliminate the adverse effect of time delay from the Lyapunov–Krasovskii function [19]. In [20], the adaptive tracking control technique has been investigated for a more general class of systems with stochastic nonlinear time delay and with a dead area at input.

In [21], by combining the adaptive neural network and backstepping technologies, a method for controlling a class of stochastic nonlinear systems that can consider uncertainty and work in the operational situation of the system is proposed. Additionally, via the combination of these two technologies, a control method for a class of strict-feedback stochastic nonlinear systems is presented in [22]. In this method, the input disturbances are also considered. In [23], a comparative adaptive neural controller has been used to design a decentralized H_∞ controller. Each of the subsystems of this proposed design are designed using the backstepping and Lyapunov methods. Recently, type-2 and-3 fuzzy systems have played a huge role in controlling the system and, as such, are proposed for a class of uncertain nonlinear systems. [24].

The innovations of this article are as follows:

- 1- Using the combination of a type-3 fuzzy neural network and a backstepping control method for the first time.
- 2- Applying actuator failure to stochastic nonlinear system in a new way.
- 3- Ensuring the stability of the control system analytically.

The structure of the article is such that the problem is explained first. Then, the specifications of type-3 fuzzy neural network are presented. The proposed control system is described in detail below. In the simulation section, the performance of the control system is evaluated. Finally, in the conclusion section, all of the research results are expressed.

2. Statement of the Problem

Consider a nonlinear stochastic strict feedback system:

$$\left\{ \begin{array}{l} dx_1 = (g_1x_2 + f_1)dt + \psi_1d\psi, \\ \vdots \\ dx_i = (g_ix_{i+1} + f_i)dt + \psi_id\psi, \\ \vdots \\ dx_n = (g_nu + f_n)dt + \psi_nd\psi, \\ y = x_1, \\ u(t) = p_0v(t) - d[v](t), \end{array} \right. \quad b_m \leq g_i \leq b_M, \quad x = [x_1, x_2, \dots, x_n]^T, \quad 1 \leq i \leq n \quad (1)$$

where ψ is the standard two-dimensional external motions defined on the probability space (Ω, F, P) with Ω as the sample space, F as a filtration, P as a criterion Probability, and smoothly unknown functions such as below:

$$f_i(\cdot), g_i(\cdot) : R^i \times R^+ \rightarrow R, \quad \psi_i^T : R^i \times R^+ \rightarrow R^{i \times i}, \quad (2)$$

where

$$f(0) = 0, \quad \psi_i^T(0) = 0 \quad (3)$$

It should be noted that in (1), u is the control input or the output of the actuator, which can be exposed to many nonlinear variations, including residuals in the actuator. In conducting this research, and in each step of the stability analysis procedure, a series of definitions, concepts, and lemma will be used, which will be briefly explained as we continue. Consider the following stochastic system:

$$dx = f(x, t)dt + h(x, t)d\psi, \quad x = [x_1, x_2, \dots, x_n]^T \in R^n \quad (4)$$

where x is vector of system state. The following factions are locally Lipchitz functions;

$$f : R^n \times R^+ \rightarrow R^n, \quad h : R^n \times R^+ \rightarrow R^{n \times r}, \quad f(0, t), \quad h(0, t) = 0, \forall t \geq 0 \quad (5)$$

Definition 1. For each function as follows:

$$V(x, t) \in C^{2,1}(R^n \times R^+, R^+) \quad (6)$$

Related to relation (4), the differential actuator L is defined as:

$$LV = \frac{\partial v}{\partial t} + \frac{\partial v}{\partial x}f + \frac{1}{2}Tr \left\{ h^T \frac{\partial^2 v}{\partial x^2} h \right\} \quad (7)$$

The last term of (7) is called an Ito correction. The second order derivative $\frac{\partial^2 v}{\partial x^2}$ is the main challenge for the control system designer and the difference between stochastic and deterministic systems is determined in this phrase.

Lemma 1. Consider a stochastic system (4), and assume that $f(x, t)$ and $h(x, t)$ in their arguments C^1 , $f(0, t)$, and $h(0, t)$ are uniformly bounded in t . In the following functions:

$$V(x, t) \in C^{2,1}(R^n \times R^+, R^+), \quad \mu(\cdot), \mu_2(\cdot) \in K_\infty \quad (8)$$

And there are the constants $a_0 > 0, b_0 \geq 0$ such that:

$$\mu_1(|x|) \leq v(x, t) \leq \mu_2(|x|), \quad LV \leq a_0v(x, t) + b_0 \quad (9)$$

Then the system (4) is bounded in probability.

Lemma 2. An inequality will also be widely used during the design of the controller and to prove its stability, hence, it is first described as an inequality.

$$xy \leq \frac{a^p}{p} [x]^p + \frac{1}{qa^q} [y]^q, (p - 1)(q - 1) = 1 \tag{10}$$

Optimal determination of values p and q is very important. Trial and error methods are commonly used in articles. In this paper, for the first time, we calculate these parameters online using a fuzzy system. This is one of the valuable innovations of this paper.

Lemma 3. For each continuous function:

$$f(x) : R^n \rightarrow R, f(0) = 0, x = [x_1, x_2, \dots, x_n]^T \tag{11}$$

with always positive functions

$$h_i(x_i)R \rightarrow R^+, j = 1, 2, \dots, n \tag{12}$$

There is

$$|f(x)| \leq \sum_{j=1}^n |x_j| h_j(x_j) \tag{13}$$

Executor actuator: analytically, suppose $C_m[0, t_E]$ is a space of uniform continuous fragment functions. For an input $v(t)$, where $v(t) \in C_m[0, t_E]$, the executable actuator is:

$$\begin{aligned} F_r[v; u_{-1}](0) &= f_r(v(0), u_{-1}) \\ F_r[v; u_{-1}](t) &= f_r(v(t), f_r[v; u_{-1}](t_1)), t_i < t \leq t_{i+1}, 0 \leq i \leq N - 1 \end{aligned} \tag{14}$$

where,

$$f_1(v, u) = \max(v - r, \min(v + r, u)) \tag{15}$$

and,

$$0 = t_0 < t_1 < \dots < t_N = t_E, \tag{16}$$

Therefore, there is a fraction in interval $[0, t_E]$, such that the function $v(t)$ on each of the sub-intervals $[t_i, t_{i+1}]$ is uniform.

Prandtl–Ishlinskii (PI) Waste: It is a nonlinear condition as follows:

$$u(t) = p_0 v(t) - \int_0^R p(r) f_r[v](t) dr \tag{17}$$

In which $u(t)$ is the output of the actuator, $v(t)$ the input signal to the actuator. $p(r)$ is the density function, and

$$p_0 = \int_0^R p(r) dr \tag{18}$$

is a constant that depends on the density function $p(r)$.

3. Type-3 Fuzzy Neural Network

In this section, the type-3 fuzzy neural network structure (Figure 1) and calculations are presented. The membership degree of type-3 fuzzy sets is calculated as follows:

$$\bar{\mu}_{\tilde{S}_T^j|\bar{\alpha}_h}(T) = \exp\left(-\frac{\left(T - c_{\tilde{S}_T^j|\bar{\alpha}_h}\right)^2}{\bar{\sigma}_{\tilde{S}_T^j|\bar{\alpha}_h}^2}\right), \bar{\mu}_{\tilde{S}_T^j|\underline{\alpha}_h}(T) = \exp\left(-\frac{\left(T - c_{\tilde{S}_T^j|\underline{\alpha}_h}\right)^2}{\bar{\sigma}_{\tilde{S}_T^j|\underline{\alpha}_h}^2}\right) \tag{19}$$

$$\mu_{\tilde{S}_T|\bar{\alpha}_h}^j(T) = \exp\left(-\frac{\left(T - c_{\tilde{S}_T|\bar{\alpha}_h}^j\right)^2}{\sigma_{\tilde{S}_T|\bar{\alpha}_h}^2}\right), \mu_{\tilde{S}_T|\underline{\alpha}_h}^j(T) = \exp\left(-\frac{\left(T - c_{\tilde{S}_T|\underline{\alpha}_h}^j\right)^2}{\sigma_{\tilde{S}_T|\underline{\alpha}_h}^2}\right) \quad (20)$$

where, $h = 1, \dots, n, j = 1, 2, c_{\tilde{S}_T|\bar{\alpha}_h}^j$ is the mean of MF $\tilde{S}_T|\bar{\alpha}_h$, $\sigma_{\tilde{S}_T|\bar{\alpha}_h}^j$, and $\sigma_{\tilde{S}_T|\underline{\alpha}_h}^j$ are the upper and lower standard divisions for $\tilde{S}_T|\bar{\alpha}_h$.

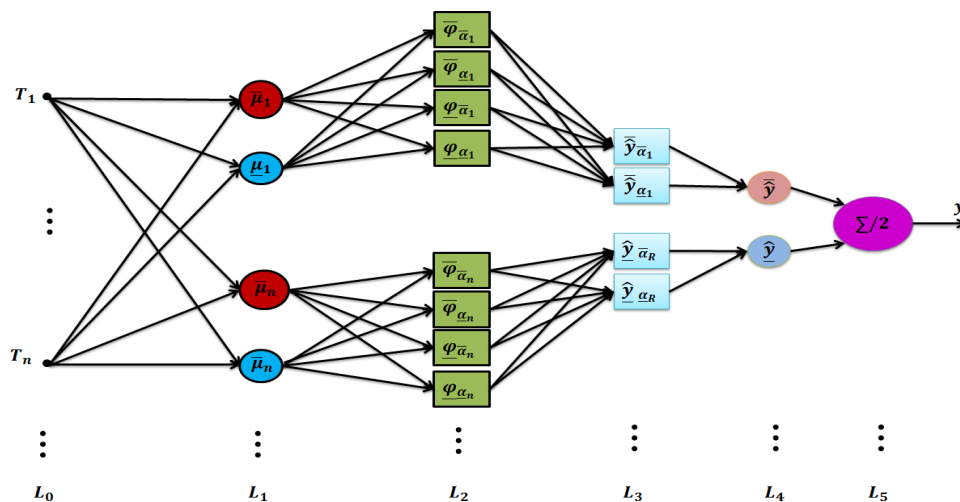


Figure 1. The structure of the type-3 fuzzy neural network.

The calculation of upper rule firing at $\bar{\alpha}_h$ are as follows:

$$\bar{\varphi}_{\bar{\alpha}_h}^1 = \bar{\mu}_{\tilde{S}_T|\bar{\alpha}_h} \bar{\mu}_{\tilde{S}_P|\bar{\alpha}_h} \bar{\mu}_{\tilde{S}_M|\bar{\alpha}_h}, \bar{\varphi}_{\bar{\alpha}_h}^2 = \bar{\mu}_{\tilde{S}_T|\bar{\alpha}_h} \bar{\mu}_{\tilde{S}_P|\bar{\alpha}_h} \bar{\mu}_{\tilde{S}_M^2|\bar{\alpha}_h} \quad (21)$$

$$\bar{\varphi}_{\bar{\alpha}_h}^3 = \bar{\mu}_{\tilde{S}_T|\bar{\alpha}_h} \bar{\mu}_{\tilde{S}_P^2|\bar{\alpha}_h} \bar{\mu}_{\tilde{S}_M|\bar{\alpha}_h}, \bar{\varphi}_{\bar{\alpha}_h}^4 = \bar{\mu}_{\tilde{S}_T|\bar{\alpha}_h} \bar{\mu}_{\tilde{S}_P^2|\bar{\alpha}_h} \bar{\mu}_{\tilde{S}_M^2|\bar{\alpha}_h} \quad (22)$$

$$\bar{\varphi}_{\bar{\alpha}_h}^5 = \bar{\mu}_{\tilde{S}_T^2|\bar{\alpha}_h} \bar{\mu}_{\tilde{S}_P|\bar{\alpha}_h} \bar{\mu}_{\tilde{S}_M|\bar{\alpha}_h}, \bar{\varphi}_{\bar{\alpha}_h}^6 = \bar{\mu}_{\tilde{S}_T^2|\bar{\alpha}_h} \bar{\mu}_{\tilde{S}_P|\bar{\alpha}_h} \bar{\mu}_{\tilde{S}_M^2|\bar{\alpha}_h} \quad (23)$$

$$\bar{\varphi}_{\bar{\alpha}_h}^7 = \bar{\mu}_{\tilde{S}_T^2|\bar{\alpha}_h} \bar{\mu}_{\tilde{S}_P^2|\bar{\alpha}_h} \bar{\mu}_{\tilde{S}_M|\bar{\alpha}_h}, \bar{\varphi}_{\bar{\alpha}_h}^8 = \bar{\mu}_{\tilde{S}_T^2|\bar{\alpha}_h} \bar{\mu}_{\tilde{S}_P^2|\bar{\alpha}_h} \bar{\mu}_{\tilde{S}_M^2|\bar{\alpha}_h} \quad (24)$$

The firing of upper rule at $\underline{\alpha}_h$, are as follows:

$$\underline{\varphi}_{\underline{\alpha}_h}^1 = \bar{\mu}_{\tilde{S}_T|\underline{\alpha}_h} \bar{\mu}_{\tilde{S}_P|\underline{\alpha}_h} \bar{\mu}_{\tilde{S}_M|\underline{\alpha}_h}, \underline{\varphi}_{\underline{\alpha}_h}^2 = \bar{\mu}_{\tilde{S}_T|\underline{\alpha}_h} \bar{\mu}_{\tilde{S}_P|\underline{\alpha}_h} \bar{\mu}_{\tilde{S}_M^2|\underline{\alpha}_h} \quad (25)$$

$$\underline{\varphi}_{\underline{\alpha}_h}^3 = \bar{\mu}_{\tilde{S}_T|\underline{\alpha}_h} \bar{\mu}_{\tilde{S}_P^2|\underline{\alpha}_h} \bar{\mu}_{\tilde{S}_M|\underline{\alpha}_h}, \underline{\varphi}_{\underline{\alpha}_h}^4 = \bar{\mu}_{\tilde{S}_T|\underline{\alpha}_h} \bar{\mu}_{\tilde{S}_P^2|\underline{\alpha}_h} \bar{\mu}_{\tilde{S}_M^2|\underline{\alpha}_h} \quad (26)$$

$$\underline{\varphi}_{\underline{\alpha}_h}^5 = \bar{\mu}_{\tilde{S}_T^2|\underline{\alpha}_h} \bar{\mu}_{\tilde{S}_P|\underline{\alpha}_h} \bar{\mu}_{\tilde{S}_M|\underline{\alpha}_h}, \underline{\varphi}_{\underline{\alpha}_h}^6 = \bar{\mu}_{\tilde{S}_T^2|\underline{\alpha}_h} \bar{\mu}_{\tilde{S}_P|\underline{\alpha}_h} \bar{\mu}_{\tilde{S}_M^2|\underline{\alpha}_h} \quad (27)$$

$$\underline{\varphi}_{\underline{\alpha}_h}^7 = \bar{\mu}_{\tilde{S}_T^2|\underline{\alpha}_h} \bar{\mu}_{\tilde{S}_P^2|\underline{\alpha}_h} \bar{\mu}_{\tilde{S}_M|\underline{\alpha}_h}, \underline{\varphi}_{\underline{\alpha}_h}^8 = \bar{\mu}_{\tilde{S}_T^2|\underline{\alpha}_h} \bar{\mu}_{\tilde{S}_P^2|\underline{\alpha}_h} \bar{\mu}_{\tilde{S}_M^2|\underline{\alpha}_h} \quad (28)$$

Equations (29)–(36) are formulations of the upper and lower slices of the lower firing rules.

$$\underline{\varphi}_{\bar{\alpha}_h}^1 = \bar{\mu}_{\tilde{S}_T|\bar{\alpha}_h} \bar{\mu}_{\tilde{S}_P|\bar{\alpha}_h} \bar{\mu}_{\tilde{S}_M|\bar{\alpha}_h}, \underline{\varphi}_{\bar{\alpha}_h}^2 = \bar{\mu}_{\tilde{S}_T|\bar{\alpha}_h} \bar{\mu}_{\tilde{S}_P|\bar{\alpha}_h} \bar{\mu}_{\tilde{S}_M^2|\bar{\alpha}_h} \quad (29)$$

$$\underline{\varphi}_{\bar{\alpha}_h}^3 = \bar{\mu}_{\tilde{S}_T|\bar{\alpha}_h} \bar{\mu}_{\tilde{S}_P^2|\bar{\alpha}_h} \bar{\mu}_{\tilde{S}_M|\bar{\alpha}_h}, \underline{\varphi}_{\bar{\alpha}_h}^4 = \bar{\mu}_{\tilde{S}_T|\bar{\alpha}_h} \bar{\mu}_{\tilde{S}_P^2|\bar{\alpha}_h} \bar{\mu}_{\tilde{S}_M^2|\bar{\alpha}_h} \quad (30)$$

$$\underline{\varphi}_{\bar{\alpha}_h}^5 = \bar{\mu}_{\tilde{S}_T^2|\bar{\alpha}_h} \bar{\mu}_{\tilde{S}_P|\bar{\alpha}_h} \bar{\mu}_{\tilde{S}_M|\bar{\alpha}_h}, \underline{\varphi}_{\bar{\alpha}_h}^6 = \bar{\mu}_{\tilde{S}_T^2|\bar{\alpha}_h} \bar{\mu}_{\tilde{S}_P|\bar{\alpha}_h} \bar{\mu}_{\tilde{S}_M^2|\bar{\alpha}_h} \quad (31)$$

$$\underline{\varphi}_{\bar{\alpha}_h}^7 = \bar{\mu}_{\tilde{S}_T^2|\bar{\alpha}_h} \bar{\mu}_{\tilde{S}_P^2|\bar{\alpha}_h} \bar{\mu}_{\tilde{S}_M|\bar{\alpha}_h}, \underline{\varphi}_{\bar{\alpha}_h}^8 = \bar{\mu}_{\tilde{S}_T^2|\bar{\alpha}_h} \bar{\mu}_{\tilde{S}_P^2|\bar{\alpha}_h} \bar{\mu}_{\tilde{S}_M^2|\bar{\alpha}_h} \quad (32)$$

$$\varphi_{\alpha_h}^1 = \bar{\mu}_{\tilde{S}_T^1|\alpha_h} \bar{\mu}_{\tilde{S}_P^1|\alpha_h} \bar{\mu}_{\tilde{S}_M^1|\alpha_h}, \varphi_{\alpha_h}^2 = \bar{\mu}_{\tilde{S}_T^1|\alpha_h} \bar{\mu}_{\tilde{S}_P^1|\alpha_h} \bar{\mu}_{\tilde{S}_M^2|\alpha_h} \tag{33}$$

$$\varphi_{\alpha_h}^3 = \bar{\mu}_{\tilde{S}_T^1|\alpha_h} \bar{\mu}_{\tilde{S}_P^2|\alpha_h} \bar{\mu}_{\tilde{S}_M^1|\alpha_h}, \varphi_{\alpha_h}^4 = \bar{\mu}_{\tilde{S}_T^1|\alpha_h} \bar{\mu}_{\tilde{S}_P^2|\alpha_h} \bar{\mu}_{\tilde{S}_M^2|\alpha_h} \tag{34}$$

$$\varphi_{\alpha_h}^5 = \bar{\mu}_{\tilde{S}_T^2|\alpha_h} \bar{\mu}_{\tilde{S}_P^1|\alpha_h} \bar{\mu}_{\tilde{S}_M^1|\alpha_h}, \varphi_{\alpha_h}^6 = \bar{\mu}_{\tilde{S}_T^2|\alpha_h} \bar{\mu}_{\tilde{S}_P^1|\alpha_h} \bar{\mu}_{\tilde{S}_M^2|\alpha_h} \tag{35}$$

$$\varphi_{\alpha_h}^7 = \bar{\mu}_{\tilde{S}_T^2|\alpha_h} \bar{\mu}_{\tilde{S}_P^2|\alpha_h} \bar{\mu}_{\tilde{S}_M^1|\alpha_h}, \varphi_{\alpha_h}^8 = \bar{\mu}_{\tilde{S}_T^2|\alpha_h} \bar{\mu}_{\tilde{S}_P^2|\alpha_h} \bar{\mu}_{\tilde{S}_M^2|\alpha_h} \tag{36}$$

The type-reduction procedure from a type-3 fuzzy to a type-2 one, are computed as follows (Figure 2):

$$\bar{y}_{\bar{\alpha}_h} = \frac{\sum_{l=1}^R \bar{\varphi}_{\bar{\alpha}_h}^l \bar{\theta}_l}{\sum_{l=1}^R (\bar{\varphi}_{\bar{\alpha}_h}^l + \varphi_{\bar{\alpha}_h}^l)}, \bar{y}_{\alpha_h} = \frac{\sum_{l=1}^R \bar{\varphi}_{\alpha_h}^l \bar{\theta}_l}{\sum_{l=1}^R (\bar{\varphi}_{\alpha_h}^l + \varphi_{\alpha_h}^l)} \tag{37}$$

$$\hat{y}_{\bar{\alpha}_h} = \frac{\sum_{l=1}^R \varphi_{\bar{\alpha}_h}^l \theta_l}{\sum_{l=1}^R (\bar{\varphi}_{\bar{\alpha}_h}^l + \varphi_{\bar{\alpha}_h}^l)}, \hat{y}_{\alpha_h} = \frac{\sum_{l=1}^R \bar{\varphi}_{\alpha_h}^l \theta_l}{\sum_{l=1}^R (\varphi_{\alpha_h}^l + \varphi_{\alpha_h}^l)} \tag{38}$$

where, R is the number of rules (here $R = 5$), and θ_l and $\bar{\theta}_l$ are the parameters of the lower and upper of the l -th rule.

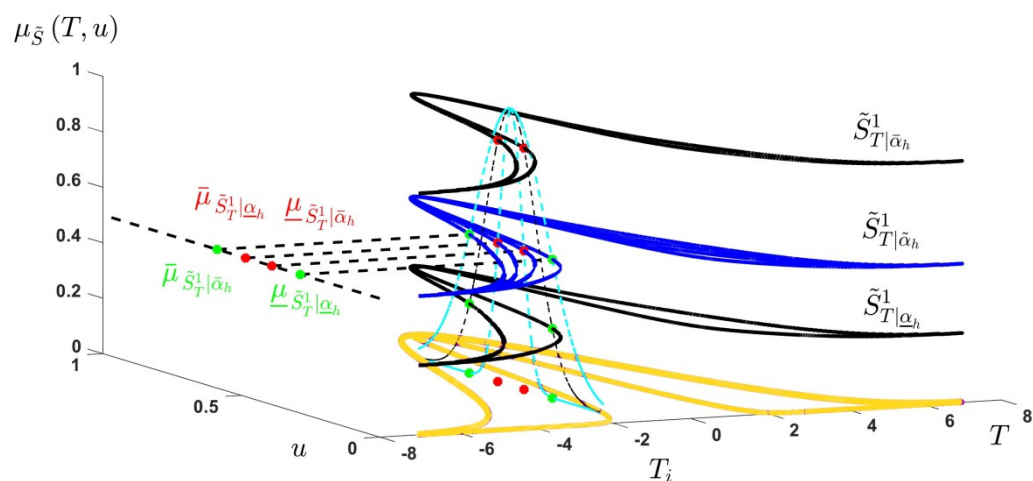


Figure 2. A view of the type-3 MF horizontal slices.

The type-reduction procedure from type-2 fuzzy to type-1 one is as follows:

$$\bar{y} = \frac{\sum_{h=1}^n \bar{\alpha}_h \bar{y}_{\bar{\alpha}_h}}{\sum_{h=1}^n (\bar{\alpha}_h + \alpha_h)} + \frac{\sum_{h=1}^n \alpha_h \bar{y}_{\alpha_h}}{\sum_{h=1}^n (\bar{\alpha}_h + \alpha_h)}, \hat{y} = \frac{\sum_{h=1}^n \bar{\alpha}_h \hat{y}_{\bar{\alpha}_h}}{\sum_{h=1}^n (\bar{\alpha}_h + \alpha_h)} + \frac{\sum_{h=1}^n \alpha_h \hat{y}_{\alpha_h}}{\sum_{h=1}^n (\bar{\alpha}_h + \alpha_h)} \tag{39}$$

The output \hat{y} is computed as:

$$\hat{y} = \frac{\bar{y} + \hat{y}}{2} \tag{40}$$

The type-3 fuzzy neural network parametric learning process can be seen in Appendix A.

4. Controller Design

As presented in the literature review, an approach for the stabilization of stochastic nonlinear systems is presented in the form of strict feedback, which is based on the back-

stepping design technique and neural networks. The present method is an extension of the method proposed in [5]. The differences between our work and the aforementioned work are as follows: replacing the backstepping design method by using the dynamic surface control (DSC) design, and the use of a type-3 fuzzy system instead of a radial base function neural network (RBFN). Numerous articles have proven the ability and accuracy of type-3 fuzzy systems compared to other computational intelligence tools. Finally, the proposed design method will be used to investigate the occurrence of PI waste in the actuator. This method is based on a multi-step recursive design algorithm that will be described below. Consider the strict feedback stochastic nonlinear system (17), then for each i step, an error surface (S_i), as follows:

$$S_i = x_i - z_i, 1 \leq i \leq n, z_1 = y_r \tag{41}$$

where S_i is the i -th error surface, x_i is the i -th state, and z_i is the i -th desired state for the system. The proposed design procedure consists of n sequential step calculations. A virtual control input \bar{x}_{i+1} for each step is defined as follows:

$$\begin{aligned} \bar{x}_{i+1} &= -k_i S_i - \frac{1}{2a_i} S_i^3 \hat{\theta} \zeta_i^T(z_i) \zeta_i(z_i), 1 \leq i \leq n, \\ z_i &= [\check{x}_i, \hat{\theta}], \check{x}_i = [x_1, \dots, x_i] \end{aligned} \tag{42}$$

$$v = \overline{\bar{x}_{n+1}} = -k_n S_n - \frac{1}{2a_n} S_n^3 \hat{\theta} \zeta_n^T(z_n) \zeta_n(z_n)$$

where k_i and a_i are the design parameters (calculated by a type-3 fuzzy system), and $\zeta_i(z_i)$ are the type-3 fuzzy membership functions in the first layer of the type-3 fuzzy neural network. An estimation of θ is shown by $\hat{\theta}$. The virtual control input is passed through a low-pass filter in order to obtain the desired value of the next step mode.

$$\epsilon_{i+1} \dot{z}_{i+1} + z_{i+1} = \bar{x}_{i+1}, 1 \leq i \leq n - 1 \tag{43}$$

In (21), ϵ_{i+1} is design parameter (calculated by type-3 fuzzy system). The i -th filter error is as follows:

$$y_i = z_i - \bar{x}_i = -\epsilon_i \dot{z}_i \tag{44}$$

The derivative of (22) is as follows:

$$dy_i = \left(\frac{y_i}{\epsilon_i} + B_i(s_i, \zeta_i, y_i, \theta, x_i, x_i) \right) dt + G_i(s_i, \zeta_i, y_i, \theta, x_i, x_i) d\psi \tag{45}$$

where $B_i(\cdot)$ and $G_i(\cdot)$ are smooth and continuous functions, with maximums of M_i and N_i , respectively. The adaptation law to update the parameters of the type-3 fuzzy neural network is as follows:

$$\hat{\theta} = \sum_{j=1}^n \frac{\lambda}{2a_j^2} S_j^6 \zeta_j^T(z_j) \zeta_j(z_j) - k_0 \hat{\theta} \tag{46}$$

The block diagram of the proposed control system is shown in Figure 3.

As shown in Figure 3, the dynamic surface control (DSC) is the main controller that needs to be configured. In previous studies that have been carried out, the parameters of this controller were usually calculated by trial and error or with prior knowledge, but in this article, we use the type-3 fuzzy neural network to calculate the aforementioned parameters. Online tuning of control system parameters is very important, especially in systems with high nonlinearity dynamics or stochastic systems, such as in [25,26].

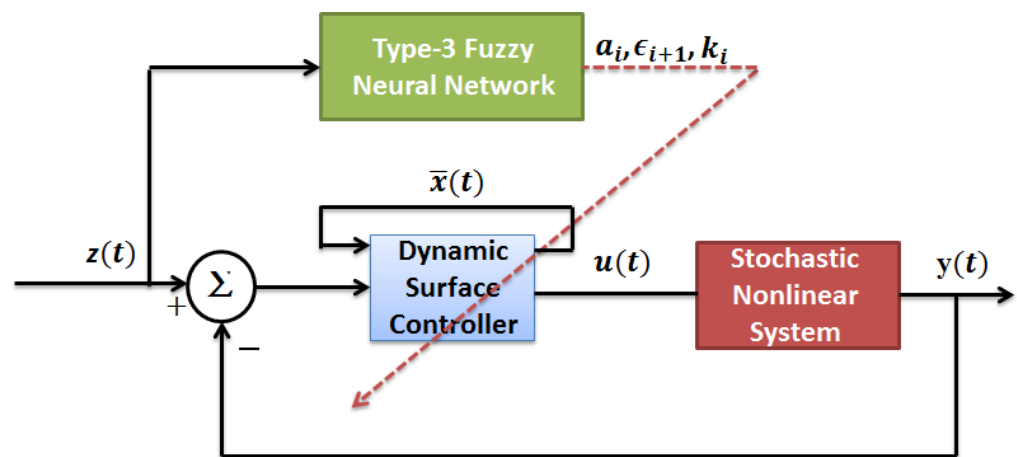


Figure 3. Block diagram of the proposed control system.

5. Simulations

In this section, to show the efficiency of the proposed method, two stochastic nonlinear dynamic systems will be controlled and the results will be depicted.

Example 1. Consider the following second-order stochastic nonlinear system.

$$\begin{cases} dx_1 = ((1 + x_1^2)x_2 + x_1 \sin(x_1))dt + x_1^3 d\psi \\ dx_2 = \left(\left(2 + \frac{x_2^2}{1+x_1^2} \right) u + x_1 x_2^2 \right) dt + (1 + \sin(x_1))x_2 d\psi \\ y = x_1 \end{cases} \quad (47)$$

where x_1 and x_2 are the states of the system, u is the input of the system (control signal), and y is the system's output. Figure 4 shows the simulation result of Example 1 and the performance of the proposed control system (dynamic surface control with a type-3 fuzzy neural network) for the convergence of both system states.

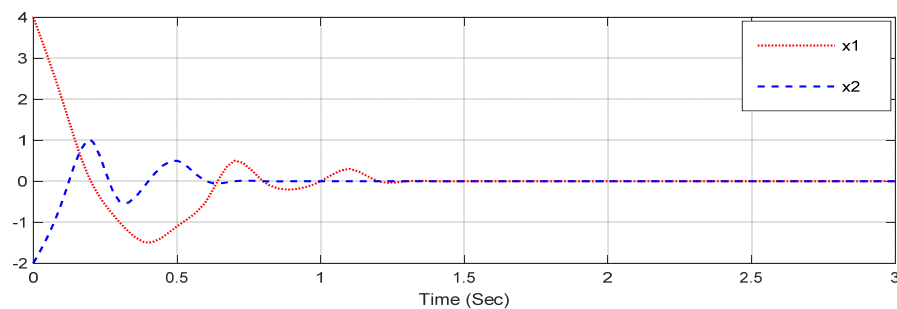


Figure 4. The states of the system (47).

The control signal generated by the proposed control system for the convergence of the states in Figure 4 is shown in Figure 5.

For further evaluation and analysis, the proposed control method is compared with the other two methods. In this scenario, the system output is supposed to rise from 0 to 5 after 1 s. One method is a dynamic surface control based on type-1 fuzzy system, and the other is based on radial basis function neural network. Figure 6 shows the result of this comparison.

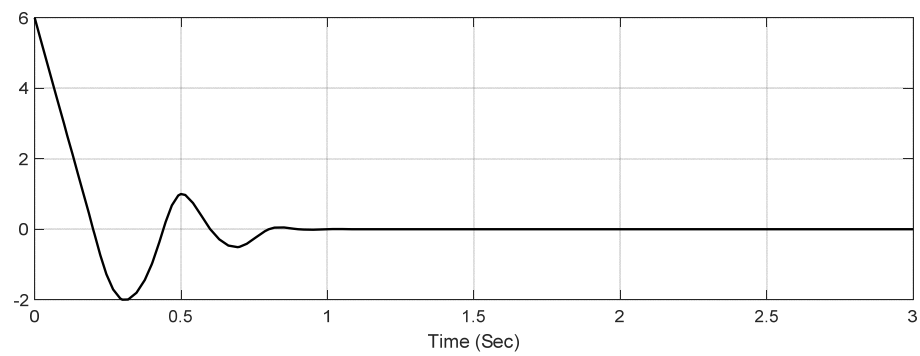


Figure 5. The control signal.

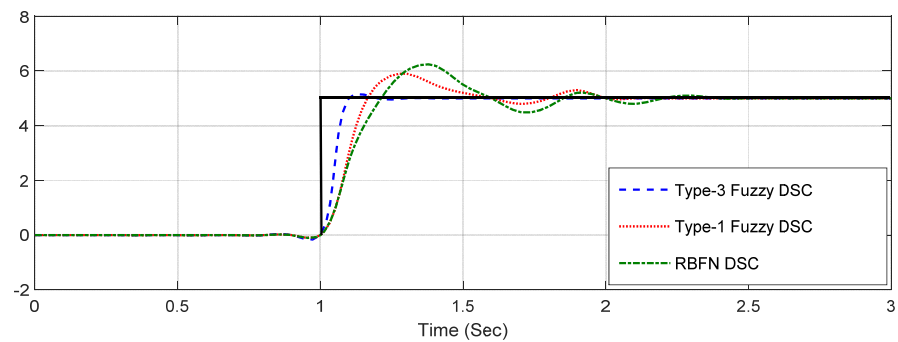


Figure 6. Comparison of dynamic surface control performance based on the type-3 fuzzy system, type-1 fuzzy system, and RBFN.

The control signals generated by all three controllers in Figure 6 are shown in Figure 7.

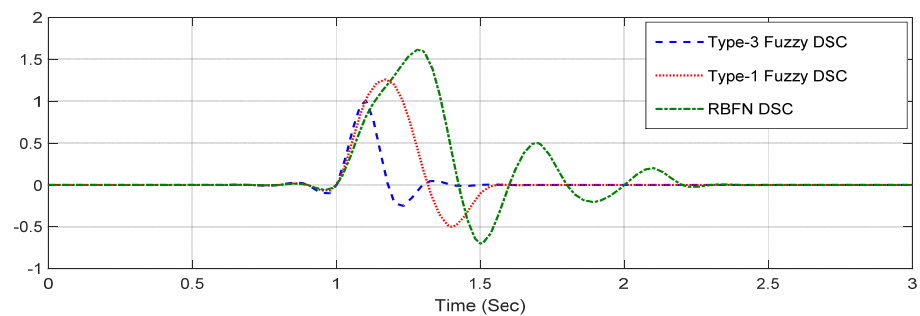


Figure 7. The control signals of the three controllers in Figure 6.

It can be seen from Figures 4–7 that the proposed control system has a good performance and has been able to manage the states (output) of the controlled system in less than 1 s. Additionally, comparison with the other two controllers (type-1 fuzzy and RBFN) shows the high speed and accuracy of the type-3 fuzzy. It can be seen from Figure 7 that the control cost (control signal peak) in the type-3 fuzzy is much lower than the other cases. In the following, a more complex system (48) is introduced, and the performance of the control system for this system (Example 2) is challenged.

Example 2. Consider the following third-order stochastic nonlinear system.

$$\begin{cases} dx_1 = ((0.3 + x_1^2)x_2 - 0.8\sin(x_1))dt + x_1\sin(x_1)d\psi \\ dx_2 = ((1 + x_2^2)x_3 - x_2 - 0.5x_2^3 - x_1^3 - \sqrt{x_1})dt + x_1\cos(x_2)d\psi \\ dx_3 = \left((1.5 + \sin(x_1x_2))x_3 - 0.5x_3 - \frac{1}{3}x_3^2 - x_2^2x_3 - \frac{x_1}{1+x_1^2} \right)dt + 3x_1e^{x_2^2}d\psi \\ y = x_1 \end{cases} \quad (48)$$

where x_1 and x_2 are the states of the system, u is the input of the system (control signal), and y is the system's output. This system (48) has three states, and the proposed control system has been able to converge all of them very well (Figure 8).

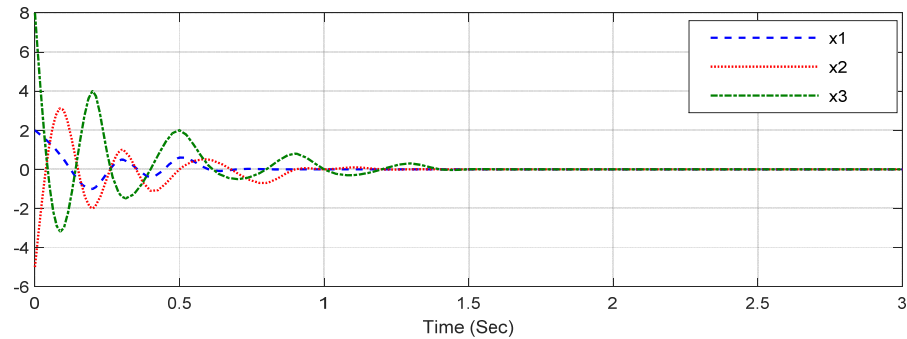


Figure 8. The control signal generated by the proposed control system is shown in Figure 9.

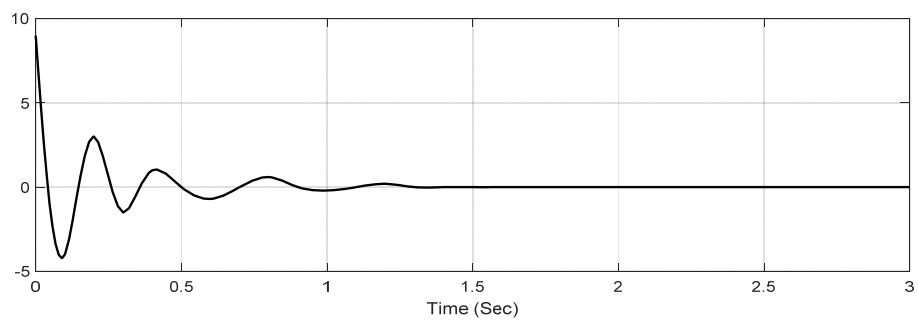


Figure 9. The control signal.

As shown in Figure 9, the control signal converges the system in less than 1.5 s. As in Example 1, here the performance of the proposed control system is compared with the other two methods, and the results are shown in Figure 10.

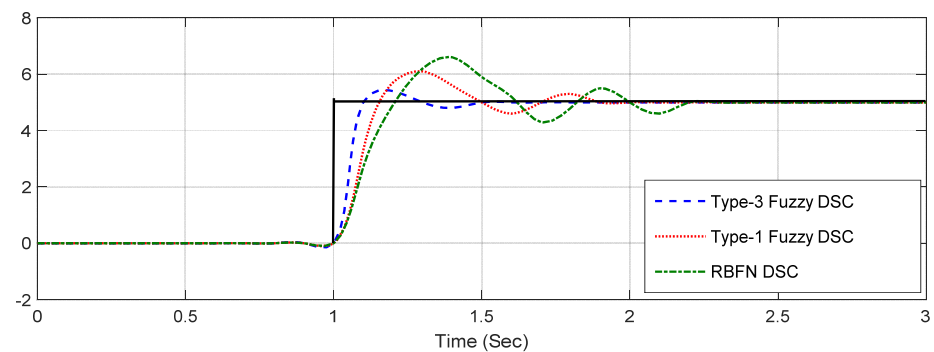


Figure 10. Comparison of dynamic surface control performance based on the type-3 fuzzy system, type-1 fuzzy system and RBFN.

It is seen in Figure 10 that the proposed control method (DSC based on a type-3 fuzzy system) manages and controls the system (48) in less than 0.5 s, while the RBFN-based method takes more than 1 s. The control signal of all three controllers for the aforementioned operation is shown in Figure 12.

As can be seen from Figures 8–12, the proposed control method has been able to handle a nonlinear and complex random system (48) well and control it in less than 1 s. Figure 10 shows that the DSC based on the type-3 fuzzy system touches the desired value for the first time in less than 0.1 s, and that the overshoot percentage is less than 6%. Additionally, Figure 11 shows a close view of Figure 10 when the step is applied. Figure 12, which shows

the control signal of all three controllers, clearly shows the fast response of the proposed method with the lowest control cost. The swirling domain of the proposed controller control signal is much lower than the RBFN DSC and type-1 fuzzy DSC methods, and its response is about 0.6 s faster than other two mentioned methods.

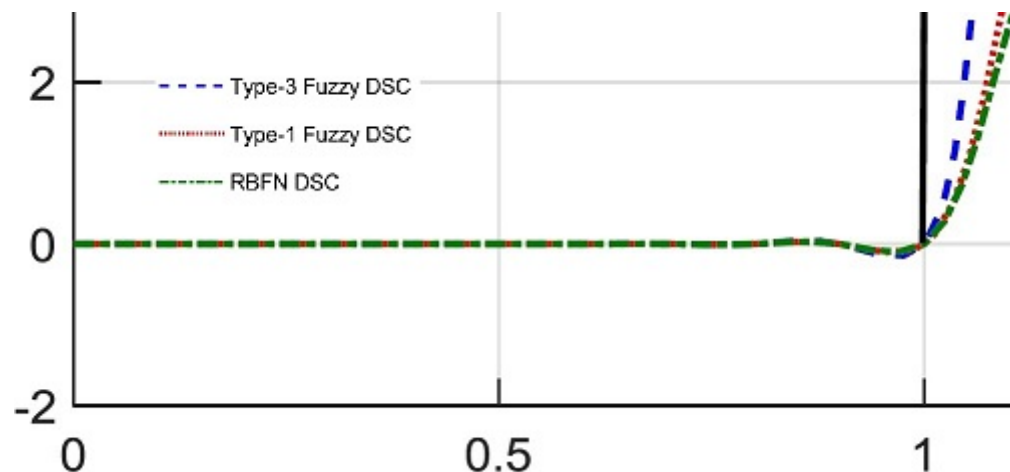


Figure 11. A closer view of Figure 10.

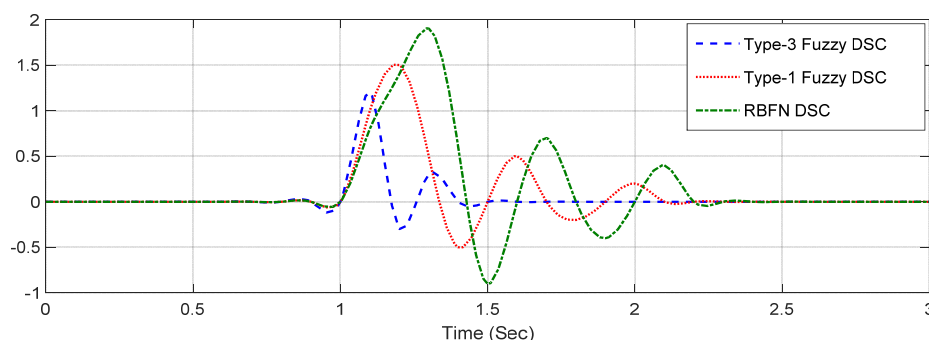


Figure 12. The control signals of the three controllers in Figure 10.

6. Conclusions

In this paper, an innovative control method for stochastic nonlinear systems is presented. In this method, for the first time, a new type-3 fuzzy system in the framework of neural networks (commonly called a type-3 fuzzy neural network) was used to adjust the dynamic surface control method. The class of stochastic nonlinear systems was considered as strict feedback with Prandtl–Ishlinskii (PI) waste, which includes a wide range of real-world systems. The proposed control system was set up to detect changes in less than 1 s, and to generate the appropriate signal immediately. To evaluate the proposed method, two common and widely used systems are simulated, and the results show the high efficiency and accuracy of the proposed control system. Additionally, to compare with other methods, two methods (a type-1 fuzzy system and RBFN) were compared with the proposed method, which testifies to the superiority of the proposed method both in terms of speed and accuracy and in terms of minimum control cost (minimum overshoot).

Author Contributions: Conceptualization, H.H., M.S. and O.M.; Data curation, H.H., J.T. and O.M.; Formal analysis, H.H., M.S. and J.T.; Funding acquisition, O.M. Investigation, H.H., M.S. and J.T.; Methodology, H.H., M.S., J.T. and O.M.; Project administration, M.S. and J.T.; Resources, H.H. and J.T.; Software, H.H. and J.T.; Supervision, H.H., J.T. and O.M.; Validation, H.H. and M.S.; Visualization, J.T.; Writing—original draft, M.S. and J.T.; Writing—review & editing, H.H., M.S. and O.M. All authors have read and agreed to the published version of the manuscript.

Funding: This research received no external funding.

Institutional Review Board Statement: Not applicable.

Informed Consent Statement: Not applicable.

Data Availability Statement: Data available on request due to restrictions e.g., privacy or ethical. The data presented in this study are available on request from the corresponding author. The data are not publicly available due to [personal reasons].

Acknowledgments: Acknowledge the Future University in Egypt (FEU) for support.

Conflicts of Interest: The authors declare no conflict of interest.

Appendix A. Learning Algorithm

In this section, the rule parameters, the centres of MFs, and the values of horizontal slices are tuned.

Appendix A.1. Tuning of Rule Parameters

The rule parameters are tuned by the EKF algorithm such that the following cost function is to be minimized:

$$J = \frac{1}{2}(y_d - \hat{y})^2 \tag{A1}$$

where y_d is the desired output and \hat{y} is the output of the suggested T3-FLS that represents the estimated output. The tuning laws for the upper and lower rule parameters $\bar{\theta}$ and $\underline{\theta}$ are given as:

$$\bar{\theta}(t) = \bar{\theta}(t - 1) + \bar{\pi}(t)\bar{\psi}(t)(y_d - \hat{y}), \underline{\theta}(t) = \underline{\theta}(t - 1) + \underline{\pi}(t)\underline{\psi}(t)(y_d - \hat{y}) \tag{A2}$$

where $\bar{\pi}$ and $\underline{\pi}(t)$ are the corresponding covariance matrices for $\bar{\theta}$ and $\underline{\theta}$, respectively. The terms $\bar{\psi}(t)$ and $\underline{\psi}(t)$ are defined as follows:

$$\bar{\psi} = [\bar{\psi}_1, \dots, \bar{\psi}_l, \dots, \bar{\psi}_R]^T, \underline{\psi} = [\underline{\psi}_1, \dots, \underline{\psi}_l, \dots, \underline{\psi}_R]^T \tag{A3}$$

where $\bar{\psi}(t)$ and $\underline{\psi}(t)$ are as follows:

$$\begin{aligned} \bar{\psi}_l &= \frac{\partial \hat{y}}{\partial \bar{\theta}_l} = \frac{\partial \hat{y}}{\partial \bar{y}} \frac{\partial \bar{y}}{\partial \bar{\theta}_l} = \frac{\partial \hat{y}}{\partial \bar{y}} \frac{\partial \bar{y}}{\partial \bar{y}_{\bar{\alpha}_h}} \frac{\partial \bar{y}_{\bar{\alpha}_h}}{\partial \bar{\theta}_l} + \frac{\partial \hat{y}}{\partial \bar{y}} \frac{\partial \bar{y}}{\partial \bar{y}_{\underline{\alpha}_h}} \frac{\partial \bar{y}_{\underline{\alpha}_h}}{\partial \bar{\theta}_l} \\ &= 0.5 \frac{1}{\sum_{h=1}^n (\bar{\alpha}_h + \underline{\alpha}_h)} \sum_{h=1}^n \bar{\alpha}_h \frac{\bar{\varphi}_{\bar{\alpha}_h}^l}{\sum_{l=1}^R (\bar{\varphi}_{\bar{\alpha}_h}^l + \varphi_{\underline{\alpha}_h}^l)} + 0.5 \frac{1}{\sum_{h=1}^n (\bar{\alpha}_h + \underline{\alpha}_h)} \sum_{h=1}^n \underline{\alpha}_h \frac{\bar{\varphi}_{\underline{\alpha}_h}^l}{\sum_{l=1}^R (\bar{\varphi}_{\bar{\alpha}_h}^l + \varphi_{\underline{\alpha}_h}^l)} \end{aligned} \tag{A4}$$

$$\begin{aligned} \underline{\psi}_l &= \frac{\partial \hat{y}}{\partial \underline{\theta}_l} = \frac{\partial \hat{y}}{\partial \bar{y}} \frac{\partial \bar{y}}{\partial \underline{\theta}_l} = \frac{\partial \hat{y}}{\partial \bar{y}} \frac{\partial \bar{y}}{\partial \bar{y}_{\bar{\alpha}_h}} \frac{\partial \bar{y}_{\bar{\alpha}_h}}{\partial \underline{\theta}_l} + \frac{\partial \hat{y}}{\partial \bar{y}} \frac{\partial \bar{y}}{\partial \bar{y}_{\underline{\alpha}_h}} \frac{\partial \bar{y}_{\underline{\alpha}_h}}{\partial \underline{\theta}_l} \\ &= 0.5 \frac{1}{\sum_{h=1}^n (\bar{\alpha}_h + \underline{\alpha}_h)} \sum_{h=1}^n \bar{\alpha}_h \frac{\varphi_{\bar{\alpha}_h}^l}{\sum_{l=1}^R (\bar{\varphi}_{\bar{\alpha}_h}^l + \varphi_{\underline{\alpha}_h}^l)} + 0.5 \frac{1}{\sum_{h=1}^n (\bar{\alpha}_h + \underline{\alpha}_h)} \sum_{h=1}^n \underline{\alpha}_h \frac{\varphi_{\underline{\alpha}_h}^l}{\sum_{l=1}^R (\bar{\varphi}_{\bar{\alpha}_h}^l + \varphi_{\underline{\alpha}_h}^l)} \end{aligned} \tag{A5}$$

Appendix A.2. Tuning of MF Parameters

For the antecedent parameters, the centres of MFs are tuned on the basis of the gradient descent method. Then the tuning laws are written as follows:

$$c_{\bar{S}_T^j}(t) = c_{\bar{S}_T^j}(t - 1) - \gamma \frac{\partial J}{\partial c_{\bar{S}_T^j}}, j = 1, 2 \tag{A6}$$

$$c_{\underline{S}_P^j}(t) = c_{\underline{S}_P^j}(t - 1) - \gamma \frac{\partial J}{\partial c_{\underline{S}_P^j}}, j = 1, 2 \tag{A7}$$

$$c_{\bar{S}_M^j}(t) = c_{\bar{S}_M^j}(t-1) - \gamma \frac{\partial J}{\partial c_{\bar{S}_M^j}}, j = 1, 2 \tag{A8}$$

where γ is the training rate. $\partial J / \partial c_{\bar{S}_T^1}$ is obtained as follows:

$$\begin{aligned} \frac{\partial J}{\partial c_{\bar{S}_T^1}} &= \frac{\partial J}{\partial \bar{y}} \frac{\partial \bar{y}}{\partial \bar{y}_{\bar{\alpha}_h}} \frac{\partial \bar{y}}{\partial \bar{y}_{\alpha_h}} \left(\sum_{l=1}^R \bar{\zeta}_T^l \frac{\partial \bar{y}_{\bar{\alpha}_h}}{\partial \bar{\varphi}_{\bar{\alpha}_h}^l} \frac{\partial \bar{\varphi}_{\bar{\alpha}_h}^l}{\partial c_{\bar{S}_T^1}} + \sum_{l=1}^R \bar{\zeta}_T^l \frac{\partial \bar{y}_{\bar{\alpha}_h}}{\partial \varphi_{\bar{\alpha}_h}^l} \frac{\partial \varphi_{\bar{\alpha}_h}^l}{\partial c_{\bar{S}_T^1}} \right) + \\ &= \frac{\partial J}{\partial \bar{y}} \frac{\partial \bar{y}}{\partial \bar{y}_{\bar{\alpha}_h}} \frac{\partial \bar{y}}{\partial \bar{y}_{\alpha_h}} \left(\sum_{l=1}^R \bar{\zeta}_T^l \frac{\partial \bar{y}_{\alpha_h}}{\partial \bar{\varphi}_{\alpha_h}^l} \frac{\partial \bar{\varphi}_{\alpha_h}^l}{\partial c_{\bar{S}_T^1}} + \sum_{l=1}^R \bar{\zeta}_T^l \frac{\partial \bar{y}_{\alpha_h}}{\partial \varphi_{\alpha_h}^l} \frac{\partial \varphi_{\alpha_h}^l}{\partial c_{\bar{S}_T^1}} \right) + \\ &= \frac{\partial J}{\partial \bar{y}} \frac{\partial \bar{y}}{\partial \bar{y}_{\bar{\alpha}_h}} \frac{\partial \bar{y}}{\partial \bar{y}_{\alpha_h}} \left(\sum_{l=1}^R \bar{\zeta}_T^l \frac{\partial \bar{y}_{\bar{\alpha}_h}}{\partial \bar{\varphi}_{\bar{\alpha}_h}^l} \frac{\partial \bar{\varphi}_{\bar{\alpha}_h}^l}{\partial c_{\bar{S}_T^1}} + \sum_{l=1}^R \bar{\zeta}_T^l \frac{\partial \bar{y}_{\bar{\alpha}_h}}{\partial \varphi_{\bar{\alpha}_h}^l} \frac{\partial \varphi_{\bar{\alpha}_h}^l}{\partial c_{\bar{S}_T^1}} \right) + \\ &= \frac{\partial J}{\partial \bar{y}} \frac{\partial \bar{y}}{\partial \bar{y}_{\bar{\alpha}_h}} \frac{\partial \bar{y}}{\partial \bar{y}_{\alpha_h}} \left(\sum_{l=1}^R \bar{\zeta}_T^l \frac{\partial \bar{y}_{\bar{\alpha}_h}}{\partial \bar{\varphi}_{\bar{\alpha}_h}^l} \frac{\partial \bar{\varphi}_{\bar{\alpha}_h}^l}{\partial c_{\bar{S}_T^1}} + \sum_{l=1}^R \bar{\zeta}_T^l \frac{\partial \bar{y}_{\bar{\alpha}_h}}{\partial \varphi_{\bar{\alpha}_h}^l} \frac{\partial \varphi_{\bar{\alpha}_h}^l}{\partial c_{\bar{S}_T^1}} \right) \end{aligned} \tag{A9}$$

where $\bar{\zeta}_T^l$ represents the l -th element of vector $\bar{\zeta}_T$. The vector $\bar{\zeta}_T$ is defined as follows:

$$\bar{\zeta}_T = [1, 1, 1, 1, 0, 0, 0, 0] \tag{A10}$$

where the elements of $\bar{\zeta}_T$ in the rules that include $c_{\bar{S}_T^1}$, are one. The terms $\frac{\partial \bar{y}_{\bar{\alpha}_h}}{\partial \bar{\varphi}_{\bar{\alpha}_h}^l}, \frac{\partial \bar{y}_{\bar{\alpha}_h}}{\partial \varphi_{\bar{\alpha}_h}^l}, \frac{\partial \bar{y}_{\alpha_h}}{\partial \bar{\varphi}_{\alpha_h}^l},$

$\frac{\partial \bar{y}_{\alpha_h}}{\partial \varphi_{\alpha_h}^l},$ and $\frac{\partial \bar{y}_{\bar{\alpha}_h}}{\partial \varphi_{\bar{\alpha}_h}^l}$ are obtained as:

$$\frac{\partial \bar{y}_{\bar{\alpha}_h}}{\partial \bar{\varphi}_{\bar{\alpha}_h}^l} = \bar{\theta}_l \frac{\sum_{l=1}^R (\bar{\varphi}_{\bar{\alpha}_h}^l + \varphi_{\bar{\alpha}_h}^l) - \bar{\varphi}_{\bar{\alpha}_h}^l}{\left(\sum_{l=1}^R (\bar{\varphi}_{\bar{\alpha}_h}^l + \varphi_{\bar{\alpha}_h}^l) \right)^2}, \frac{\partial \bar{y}_{\bar{\alpha}_h}}{\partial \varphi_{\bar{\alpha}_h}^l} = \bar{\theta}_l \frac{-1}{\left(\sum_{l=1}^R (\bar{\varphi}_{\bar{\alpha}_h}^l + \varphi_{\bar{\alpha}_h}^l) \right)^2} \tag{A11}$$

$$\frac{\partial \bar{y}_{\alpha_h}}{\partial \bar{\varphi}_{\alpha_h}^l} = \bar{\theta}_l \frac{\sum_{l=1}^R (\bar{\varphi}_{\alpha_h}^l + \varphi_{\alpha_h}^l) - \bar{\varphi}_{\alpha_h}^l}{\left(\sum_{l=1}^R (\bar{\varphi}_{\alpha_h}^l + \varphi_{\alpha_h}^l) \right)^2}, \frac{\partial \bar{y}_{\alpha_h}}{\partial \varphi_{\alpha_h}^l} = \bar{\theta}_l \frac{-1}{\left(\sum_{l=1}^R (\bar{\varphi}_{\alpha_h}^l + \varphi_{\alpha_h}^l) \right)^2} \tag{A12}$$

$$\frac{\partial \bar{y}_{\bar{\alpha}_h}}{\partial \varphi_{\bar{\alpha}_h}^l} = \bar{\theta}_l \frac{\sum_{l=1}^R (\bar{\varphi}_{\bar{\alpha}_h}^l + \varphi_{\bar{\alpha}_h}^l) - \bar{\varphi}_{\bar{\alpha}_h}^l}{\left(\sum_{l=1}^R (\bar{\varphi}_{\bar{\alpha}_h}^l + \varphi_{\bar{\alpha}_h}^l) \right)^2}, \frac{\partial \bar{y}_{\bar{\alpha}_h}}{\partial \bar{\varphi}_{\bar{\alpha}_h}^l} = \bar{\theta}_l \frac{-1}{\left(\sum_{l=1}^R (\bar{\varphi}_{\bar{\alpha}_h}^l + \varphi_{\bar{\alpha}_h}^l) \right)^2} \tag{A13}$$

$$\frac{\partial \bar{y}_{\alpha_h}}{\partial \varphi_{\alpha_h}^l} = \bar{\theta}_l \frac{\sum_{l=1}^R (\bar{\varphi}_{\alpha_h}^l + \varphi_{\alpha_h}^l) - \bar{\varphi}_{\alpha_h}^l}{\left(\sum_{l=1}^R (\bar{\varphi}_{\alpha_h}^l + \varphi_{\alpha_h}^l) \right)^2}, \frac{\partial \bar{y}_{\alpha_h}}{\partial \bar{\varphi}_{\alpha_h}^l} = \bar{\theta}_l \frac{-1}{\left(\sum_{l=1}^R (\bar{\varphi}_{\alpha_h}^l + \varphi_{\alpha_h}^l) \right)^2} \tag{A14}$$

For $\frac{\partial \bar{\varphi}_{\bar{\alpha}_h}^l}{\partial c_{\bar{S}_T^1}}, \frac{\partial \varphi_{\bar{\alpha}_h}^l}{\partial c_{\bar{S}_T^1}}, \frac{\partial \bar{\varphi}_{\alpha_h}^l}{\partial c_{\bar{S}_T^1}},$ and $\frac{\partial \varphi_{\alpha_h}^l}{\partial c_{\bar{S}_T^1}}$ one has:

$$\frac{\partial \bar{\varphi}_{\bar{\alpha}_h}^l}{\partial c_{\bar{S}_T^1}} = \frac{2(T - c_{\bar{S}_T^1|\bar{\alpha}_h})}{\bar{\sigma}_{\bar{S}_T^1|\bar{\alpha}_h}^2} \bar{\varphi}_{\bar{\alpha}_h}^l, \frac{\partial \varphi_{\bar{\alpha}_h}^l}{\partial c_{\bar{S}_T^1}} = \frac{2(T - c_{\bar{S}_T^1|\alpha_h})}{\bar{\sigma}_{\bar{S}_T^1|\alpha_h}^2} \varphi_{\bar{\alpha}_h}^l \tag{A15}$$

$$\frac{\partial \bar{\varphi}_{\alpha_h}^l}{\partial c_{\bar{S}_T^1}} = \frac{2(T - c_{\bar{S}_T^1|\bar{\alpha}_h})}{\bar{\sigma}_{\bar{S}_T^1|\bar{\alpha}_h}^2} \bar{\varphi}_{\alpha_h}^l, \frac{\partial \varphi_{\alpha_h}^l}{\partial c_{\bar{S}_T^1}} = \frac{2(T - c_{\bar{S}_T^1|\alpha_h})}{\bar{\sigma}_{\bar{S}_T^1|\alpha_h}^2} \varphi_{\alpha_h}^l \tag{A16}$$

The computation for terms $\partial J/\partial c_{\tilde{S}_T^2}$, $\partial J/\partial c_{\tilde{S}_M^1}$, $\partial J/\partial c_{\tilde{S}_M^2}$, $\partial J/\partial c_{\tilde{S}_P^1}$ and $\partial J/\partial c_{\tilde{S}_P^2}$, are the same as $\partial J/\partial c_{\tilde{S}_T^1}$, with difference that $\bar{\zeta}_T$ is repealed with $\underline{\zeta}_T$, $\bar{\zeta}_M$, $\underline{\zeta}_M$, $\bar{\zeta}_P$, and $\underline{\zeta}_P$, respectively. Additionally, terms $c_{\tilde{S}_T^1|\bar{\alpha}_h}$, $c_{\tilde{S}_T^1|\underline{\alpha}_h}$, $\bar{\sigma}_{\tilde{S}_T^1|\bar{\alpha}_h}$ and $\bar{\sigma}_{\tilde{S}_T^1|\underline{\alpha}_h}^2$ should be replaced with the corresponding terms. The vectors $\underline{\zeta}_T$, $\bar{\zeta}_M$, $\underline{\zeta}_M$, $\bar{\zeta}_P$, and $\underline{\zeta}_P$ are defined as follows:

$$\underline{\zeta}_T = [0, 0, 0, 0, 1, 1, 1, 1], \bar{\zeta}_M = [1, 0, 1, 0, 1, 0, 1, 0] \tag{A17}$$

$$\underline{\zeta}_M = [0, 1, 0, 1, 0, 1, 0, 1], \bar{\zeta}_P = [1, 1, 0, 0, 1, 1, 0, 0], \underline{\zeta}_P = [0, 0, 1, 1, 0, 0, 1, 1] \tag{A18}$$

Table A1. Explaining the symbols used in this paper.

Symbol	Description	Symbol	Description
ψ	standard 2-dimensional external motions	F	filtration
P	criterion Probability	X	vector of system state
$C_m[0, t_E]$	space of uniform continuous fragment functions	$u(t)$	output of the actuator
$v(t)$	input signal to the actuator	$p(r)$	density function
$\bar{\sigma}_{\tilde{S}_T^j \bar{\alpha}_h}$	upper standard divisions for $\tilde{S}_T^j \bar{\alpha}_h$	$\sigma_{\tilde{S}_T^j \bar{\alpha}_h}$	lower standard divisions for $\tilde{S}_T^j \bar{\alpha}_h$
θ_i	parameters of lower of l -th rule	$\bar{\theta}_i$	parameters of upper of l -th rule
S_i	i -th error surface	x_i	i -th state
z_i	i -th desired state for the system	k_i	design parameters
a_i	design parameters	$\zeta_i(z_i)$	type-3 fuzzy membership functions in the first layer of the type-3 fuzzy neural network
ϵ_{i+1}	design parameter	$B_i(\cdot)$	smooth functions
$G_i(\cdot)$	continue functions	M_i	smooth functions maximum
N_i	continue functions maximum	u	input of the system (control signal)
y	system's output	$\bar{\pi}$	corresponding covariance matrices for $\bar{\theta}$

References

- Vaiana, N.; Sessa, S.; Marmo, F.; Rosati, L. A class of uniaxial phenomenological models for simulating hysteretic phenomena in rate-independent mechanical systems and materials. *Nonlinear Dyn.* **2018**, *93*, 1647–1669. [CrossRef]
- Vaiana, N.; Sessa, S.; Rosati, L. A generalized class of uniaxial rate-independent models for simulating asymmetric mechanical hysteresis phenomena. *Mech. Syst. Signal Process.* **2021**, *146*, 106984. [CrossRef]
- Aguirre, G.; Janssens, T.; Brussel, H.V.; Al-Bender, F. Asymmetric-hysteresis compensation in piezoelectric actuators. *Mech. Syst. Signal Process.* **2012**, *30*, 218–231. [CrossRef]
- Borisov, A.; Bosov, A.; Miller, A. Optimal Stabilization of Linear Stochastic System with Statistically Uncertain Piecewise Constant Drift. *Mathematics* **2022**, *10*, 184. [CrossRef]
- Bashkirtseva, I. Controlling Stochastic Sensitivity by Feedback Regulators in Nonlinear Dynamical Systems with Incomplete Information. *Mathematics* **2021**, *9*, 3229. [CrossRef]
- Tavoosi, J.; Shirkhani, M.; Abdali, A.; Mohammadzadeh, A.; Nazari, M.; Mobayen, S.; Asad, J.H.; Bartoszewicz, A. A New General Type-2 Fuzzy Predictive Scheme for PID Tuning. *Appl. Sci.* **2021**, *11*, 10392. [CrossRef]
- Wang, J.; Xu, C.; Tavoosi, J. A Novel Nonlinear Control for Uncertain Polynomial Type-2 Fuzzy Systems (Case Study: Cart-Pole System). *Int. J. Uncertain. Fuzziness Knowl.-Based Syst.* **2021**, *29*, 753–770. [CrossRef]
- Mohammadi, F.; Mohammadi-ivatloo, B.; Gharehpetian, G.B.; Ali, M.H.; Wei, W.; Erdinç, O.; Shirkhani, M. Robust Control Strategies for Microgrids: A Review. *IEEE Syst. J.* **2021**, 1–12. [CrossRef]
- Wang, M.; Wang, Z.; Dong, H.; Han, Q.L. A Novel Framework for Backstepping-Based Control of Discrete-Time Strict-Feedback Nonlinear Systems with Multiplicative Noises. *IEEE Trans. Autom. Control* **2021**, *66*, 1484–1496. [CrossRef]
- Zhang, H.; Zhang, X.; Bu, R. Radial Basis Function Neural Network Sliding Mode Control for Ship Path Following Based on Position Prediction. *J. Mar. Sci. Eng.* **2021**, *9*, 1055. [CrossRef]
- Niu, B.; Li, H.; Zhang, Z.; Li, J.; Hayat, T.; Alsaadi, F.E. Adaptive Neural-Network-Based Dynamic Surface Control for Stochastic Interconnected Nonlinear Nonstrict-Feedback Systems with Dead Zone. *IEEE Trans. Syst. Man Cybern. Syst.* **2019**, *49*, 1386–1398. [CrossRef]
- O'Hara, J.M.; Jolly, J.C.K.; Reynold, C.E.; Mantis, N.J. Localization of non-linear neutralizing B cell epitopes on ricin toxin's enzymatic subunit (RTA). *Immunol. Lett.* **2014**, *158*, 7–13. [CrossRef] [PubMed]

13. Labiod, S.; Guerra, T.M. Adaptive Fuzzy Control for Multivariable Nonlinear Systems with Indefinite Control Gain Matrix and Unknown Control Direction. *IFAC-PapersOnLine* **2020**, *53*, 8019–8024. [[CrossRef](#)]
14. Fei, J.; Fang, Y.; Yuan, Z. Adaptive Fuzzy Sliding Mode Control for a Micro Gyroscope with Backstepping Controller. *Micromachines* **2020**, *11*, 968. [[CrossRef](#)]
15. Wu, G.Q.; Song, S.M.; Sun, J.N. Finite-Time Dynamic Surface Antisaturation Control for Spacecraft Terminal Approach Considering Safety. *J. Spacecr. Rocket.* **2018**, *55*, 1430–1443. [[CrossRef](#)]
16. Ma, Z.; Ma, H. Adaptive Fuzzy Backstepping Dynamic Surface Control of Strict-Feedback Fractional-Order Uncertain Nonlinear Systems. *IEEE Trans. Fuzzy Syst.* **2020**, *28*, 122–133. [[CrossRef](#)]
17. Hu, J.; Zhang, P.; Kao, Y.; Liu, H.; Chen, D. Sliding mode control for Markovian jump repeated scalar nonlinear systems with packet dropouts: The uncertain occurrence probabilities case. *Appl. Math. Comput.* **2019**, *362*, 124574. [[CrossRef](#)]
18. Sui, S.; Chen, C.L.P.; Tong, S. Neural-Network-Based Adaptive DSC Design for Switched Fractional-Order Nonlinear Systems. *IEEE Trans. Neural Netw. Learn. Syst.* **2021**, *32*, 4703–4712. [[CrossRef](#)]
19. Sheng, Z.; Lin, C.; Chen, B.; Wang, Q.G. An asymmetric Lyapunov-Krasovskii functional method on stability and stabilization for T-S fuzzy systems with time delay. *IEEE Trans. Fuzzy Syst.* **2021**, *1*. [[CrossRef](#)]
20. Min, H.; Xu, S.; Zhang, Z. Adaptive Finite-Time Stabilization of Stochastic Nonlinear Systems Subject to Full-State Constraints and Input Saturation. *IEEE Trans. Autom. Control* **2021**, *66*, 1306–1313. [[CrossRef](#)]
21. Wang, J.; Liu, Z.; Zhang, Y.; Chen, C.L.P.; Lai, G. Adaptive Neural Control of a Class of Stochastic Nonlinear Uncertain Systems With Guaranteed Transient Performance. *IEEE Trans. Cybern.* **2020**, *50*, 2971–2981. [[CrossRef](#)] [[PubMed](#)]
22. Homayoun, B.; Arefi, M.M.; Vafamand, N. Robust adaptive backstepping tracking control of stochastic nonlinear systems with unknown input saturation: A command filter approach. *Int. J. Robust Nonlinear Control* **2020**, *30*, 3296–3313. [[CrossRef](#)]
23. Liu, H.; Li, X.; Liu, X.; Wang, H. Backstepping-based decentralized bounded- H_∞ adaptive neural control for a class of large-scale stochastic nonlinear systems. *J. Frankl. Inst.* **2019**, *356*, 8049–8079. [[CrossRef](#)]
24. Mohammadzadeh, A.; Castillo, O.; Band, S.S.; Mosavi, A. A Novel Fractional-Order Multiple-Model Type-3 Fuzzy Control for Nonlinear Systems with Unmodeled Dynamics. *Int. J. Fuzzy Syst.* **2021**, *23*, 1633–1651. [[CrossRef](#)]
25. Al-Bender, F.; Symens, W.; Swevers, J.; Brussel, H.V. Theoretical analysis of the dynamic behavior of hysteresis elements in mechanical systems. *Int. J. Non-Linear Mech.* **2004**, *39*, 1721–1735. [[CrossRef](#)]
26. Vaiana, N.; Sessa, S.; Marmo, F.; Rosati, L. Nonlinear dynamic analysis of hysteretic mechanical systems by combining a novel rate-independent model and an explicit time integration method. *Nonlinear Dyn.* **2019**, *98*, 2879–2901. [[CrossRef](#)]